ACS APPLIED POLYMER MATERIALS

pubs.acs.org/acsapm

Article

One-Step Synthesis of Gelatin-Conjugated Supramolecular Hydrogels for Dynamic Regulation of Adhesion Contact and Morphology of Myoblasts

Kentaro Hayashi, Mami Matsuda, Nodoka Mitake, Masaki Nakahata, Natalie Munding, Akira Harada, Stefan Kaufmann, Yoshinori Takashima,* and Motomu Tanaka*

Cite This: *ACS Appl. Polym. Mater.* 2022, 4, 2595−2603

Read Online

ACCESS | Metrics & More | Article Recommendations | Supporting Information

ABSTRACT: Hydrogels possessing fine-adjustable and switchable elasticity emulate the mechanical microenvironments of biological cells, which are known to change dynamically during development and disease progression. In this study, a supramolecular hydrogel conjugated with gelatin side chains was synthesized. By systematically screening the molar fraction of supramolecular host/guest cross-linkers, Young's modulus of the substrate was fine-adjusted to the level for myoblasts, $E \approx 10$ kPa. C2C12 myoblasts reproducibly and firmly adhered to the gelatin-conjugated hydrogel via focal adhesion contacts consisting of integrin clusters, whereas only a few cells adhered to the gel without gelatin side chains. The elasticity of the gelatin-conjugated hydrogel was switchable to desired levels by simply adding and removing free guest molecules in appropriate concentrations without interfering with cell viability. Immunofluorescence confocal microscopy images of fixed cells confirmed the adaptation of focal adhesions and remodeling of actin cytoskeletons on the gelatin-conjugated hydrogel. Time-lapse phase-contrast images demonstrated the dynamic response of the cells, manifested in their morphology, to an abrupt change in the substrate elasticity. Gelatin-conjugated hydrogels with switchable elasticity enable the direct and reversible mechanical stimulation of cells in one step without tedious surface functionalization with adhesion ligands.

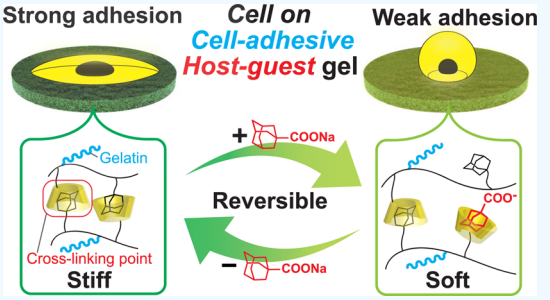

KEYWORDS: *supramolecular hydrogel, gelatin, reversible cross-links, switchable elasticity, mechanosensing*

1. INTRODUCTION

Ample evidence suggested that the fate and functions of biological cells are directed not only by biochemical factors but also by the biophysical properties of the surrounding microenvironment.[1,2] The formation of parallel acto-myosin bundles in myotubes[3] and neurite branches by neuronal cells[4] is optimal on substrates with elasticity similar to that of the native extracellular environment. Using chemically cross-linked polyacrylamide substrates coated with type I collagen, Discher and co-workers demonstrated that the differentiation of mesenchymal stem cells is directed by Young's modulus E of the substrate.[5] Studies conducted over the past two decades indicate that mechanical incompliance between cells and their environments may result in the misdirection of cell fate. For example, mesenchymal stem cells injected into a fibrotic liver differentiate into ductal cells, not hepatocytes, because a fibrotic liver is much stiffer than a healthy liver.[6] Przybyla et al. reported that human embryonic stem cells (hESCs) detect with high sensitivity the elasticity of hydrogel substrates and undergo β-catenin/Wnt-dependent mesoderm differentiation accordingly.[7]

To achieve ideal mechanical compliance between cells and contact substrates, chemically cross-linked hydrogels have been widely used as models of the extracellular matrix (ECM)[8] because Young's modulus of these hydrogels can be fine-adjusted by the cross-linker concentration and reaction time.[9,10] However, polymer networks cross-linked by covalent bonds are not able to alter the elasticity reversibly. It is well established that extracellular microenvironments are not static but highly dynamic both in space and time. The structure and mechanical properties of the ECM are significantly modulated by many diseases. For example, fibrotic stiffening of the bone marrow is characteristic of some blood cancers, such as osteomyeloma,[11] and remodeling of the ECM plays a key role in chronic obstructive pulmonary disease (COPD).[12] Moreover, many metastatic cancers are characterized by the upregulation of matrix metalloproteases that digest and modulate the mechanical properties of the ECM.[13] All these findings indicate that there is a clear demand for a new class of

Received: December 26, 2021
Accepted: February 15, 2022
Published: March 29, 2022

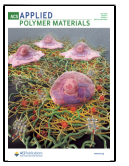

polymer materials with mechanical properties that can be modulated on demand by external cues for use as models of the ECM.

To date, a number of polymer materials that can change their mechanical properties in response to external cues, such as light, pH, temperature, and other chemical substances, have been developed.[14−20] Previously, we fabricated hydrogels based on physically cross-linked micelles of a triblock copolymer possessing pH-responsive blocks at two ends and demonstrated that the morphology and adhesion strength of C2C12 myoblast and human mesenchymal stem cells can be switched reversibly.[21−23] To switch the substrate elasticity at physiological pH, we also fabricated polyacrylamide hydrogels cross-linked with host-guest interactions[24−27] by modifying the acrylamide monomer with the host (β-cyclodextrin, βCD) and guest (adamantane, Ad) moieties. By optimizing the mixing ratio of pure acrylamide monomers (matrix) to acrylamide monomers modified with host/guest moieties, the resulting hydrogels can recapitulate the elasticity of the ECM of muscles (4−11 kPa).[26] Nevertheless, it is still necessary to functionalize their surfaces to allow cell adhesion with ECM proteins, such as collagen, laminin, and fibronectin with the aid of cross-linkers. For example, sulfosuccinimidyl 6-(4′-azido-2′-nitrophenylamino)hexanoate (sulfo-SANPAH) is one of the widely used photocross-linker to harness ECM proteins on hydrogel surfaces, but additional functionalization steps often make it difficult to reproduce cell behaviors. Herein, we report a one-step synthesis of polyacrylamide-based supramolecular hydrogels functionalized with gelatin side chains in addition to host (βCD) and guest (Ad) moieties. As we reported previously,[26] the supramolecular cross-links realize the fine-adjustment of substrate stiffness (Young's modulus) because the number of host-guest complexes changes in response to the chemical stimuli, that is, the change in [AdCOOH] in the culture medium. This allows seeding of cells directly on dynamically tunable hydrogel substrates without tedious surface functionalization. The Young's modulus and cell behavior were evaluated as functions of the molar fraction of host/guest monomers and the concentration of free 1-adamantanecarboxylic acid sodium salt (AdCOONa) in the culture medium under static conditions. Moreover, we monitored the dynamic response of the cells to abrupt changes in Young's modulus of hydrogel substrates.

2. EXPERIMENTAL SECTION

2.1. Materials. Phosphate-buffered saline (PBS), toluene, acetone, and D_2O were purchased from Wako Pure Chemical Industries, Ltd. Ethanol was purchased from Shinwa Alcohol Industry Co., Ltd. (Tokyo, Japan). 6-Acrylamidomethyl−βCD (βCD-AAmMe) was obtained from Kyoeisha Chemical Co., Ltd. (Osaka, Japan). Adamantane−acrylamide (Ad-AAm) was obtained from Yushiro Chemical Industry Co., Ltd. (Tokyo, Japan). Sodium hydroxide, acrylamide (AAm), and 2-(*N*-morpholino)ethane sulfonic acid (MES) were purchased from Nacalai Tesque Inc. (Kyoto, Japan). Lithium(2,4,6-trimethylbenzoyl)phosphinate (LAP), 1-adamantanecarboxylic acid, and vinyltrimethoxysilane were purchased from Tokyo Chemical Industry Co., Ltd. (Tokyo, Japan). Gelatin type A from porcine skin (bloom strength ∼300), methacrylic anhydride, RPMI-1640 medium, fetal bovine serum, penicillin, and streptomycin were purchased from Sigma-Aldrich, Co. (Tokyo, Japan). Water used to prepare aqueous solutions was purified using a Millipore Integral MT system (Tokyo, Japan). Unless otherwise stated, other reagents were purchased from Sigma-Aldrich and used without further purification.

2.2. Preparation of βCD-Ad-Gelatin Bulk Gels. The synthesis[28] and characterization of methacrylamide-modified gelatin are described in Supporting Information S1 and S2. Methacrylamide-modified gelatin was dissolved in PBS at 60 °C to obtain a transparent solution (1.0 w/v%). To fabricate βCD-Ad-Gelatin hydrogels, we first prepared the inclusion complex, βCD-AAmMe/Ad-AAm, as described in Supporting Information S3, and successful complex formation was confirmed using ^{1}H-^{1}H two-dimensional (2D) rotating-frame nuclear Overhauser effect spectroscopy (ROESY) NMR (Supporting Information S4). AAm (100 − 2*x* mol %) and βCD-AAmMe/Ad-AAm (2*x* mol %) were added to the methacrylamide-modified gelatin dissolved in PBS. Here, *x* represents mol % of βCD-AAmMe and Ad-AAm monomers. The total concentration of βCD-AAmMe, Ad-AAm, and AAm was 2 M (Supporting Information S5). After all the monomers were dissolved, LAP (0.02 M) was added to the PBS solution, and the reaction solution was poured into a round-shaped silicon mold (diameter: 8 mm, thickness: 2 mm) mounted on a glass substrate. The reaction solution was then illuminated for 20 min using a light-emitting diode (LED) light source device (POT-365, Asahi Spectra, Tokyo, Japan) to photoactivate polymerization (λ = 365 nm, 1.0 mW/cm^2), resulting in the formation of a bulk βCD-Ad-Gelatin gel. Finally, the sample was washed with PBS (2.5 mL) three times every 10 min and soaked in PBS (2.5 mL) for 24 h. The basic characteristics of these samples were determined, for example, the measurement of Young's modulus using a creep meter.

2.3. Preparation of βCD-Ad-Gelatin Films for Cell Culture. Because the cells cultured on βCD-Ad-Gelatin were visualized using inverted microscopes, it was necessary to control the film thickness within the order of 100 μm. For this purpose, we slightly modified the preparation steps. First, to covalently couple βCD-Ad-Gelatin to the substrate, a round cover glass (Ø = 25 mm), treated with plasma (air, 30 s) was immersed in a 5 v/v% solution of vinyltrimethoxysilane in toluene, and the sample container was shaken at 500 rpm for 18 h at room temperature. After sequential rinsing in acetone, ethanol, and deionized water, the silane-coated glass substrate was dried at 70 °C for 1 h in air and protected from ultraviolet (UV) light until final use. A 77 μL portion of methacrylamide-modified gelatin, βCD-AAmMe/Ad-AAm, and LAP in PBS solution was injected into a gap between a polyvinylidene chloride sheet and the vinyl-silanized glass substrate and irradiated with UV light (λ = 365 nm, 1.0 mW/cm^2) through the glass slide for 20 min. Prior to cell seeding, the sample was washed with PBS (2.5 mL) three times every 10 min and soaked in PBS (2.5 mL) for 24 h to remove the residual chemicals.

2.4. Physical Characterization of βCD-Ad-Gelatin. The βCD-Ad-Gelatin hydrogel (*x* = 2 as a representative sample) was characterized by ^{1}H field-gradient magic-angle-spinning (FGMAS) NMR (ECA-400WB, JEOL, Tokyo) and attenuated total reflection Fourier transform infrared (ATR-FT-IR) spectroscopy (FT/IR 6100, JASCO, Tokyo). For the FGMAS NMR, the hydrogel was dried in a 30 °C convection oven (WFO-420, EYELA, Tokyo, Japan) for 18 h, kept in vacuum overnight, and fully hydrated by D_2O. For ATR-IR, the hydrogel was dried in the 30 °C convection oven for 18 h and then crushed into powder. The FGMAS NMR and ATR FT-IR data are presented in Supporting Information S6 and S7, respectively, confirming the successful integration of gelatin in the supramolecular hydrogels. The Young's modulus of bulk βCD-Ad-Gelatin was measured using a Rheoner RE-33005 creep meter (Yamaden Ltd., Tokyo, Japan) equipped with a rod-shaped teflon plunger at a compression velocity of 0.1 mm/s. The Young's modulus *E* was calculated from the initial slope of the stress−strain curve in the range of 1−5% strain. The elasticity of βCD-Ad-Gelatin near the surface was determined via nanoindentation using an atomic force microscope (NanoWizard, JPK Instruments, Berlin, Germany). As reported previously, we indented the sample with a Pyrex-nitride spherical colloidal probe (r = 5 μm) attached to a Si_3N_4 cantilever with a nominal spring constant of 0.08 N/m (CP-PNP-BSG; Olympus, Tokyo, Japan). The Young's modulus *E* of βCD-Ad-Gelatin was calculated from the nonlinear least-squares fit of the force−indentation curves:[29,30]

https://doi.org/10.1021/acsapm.1c01902
ACS Appl. Polym. Mater. 2022, 4, 2595−2603

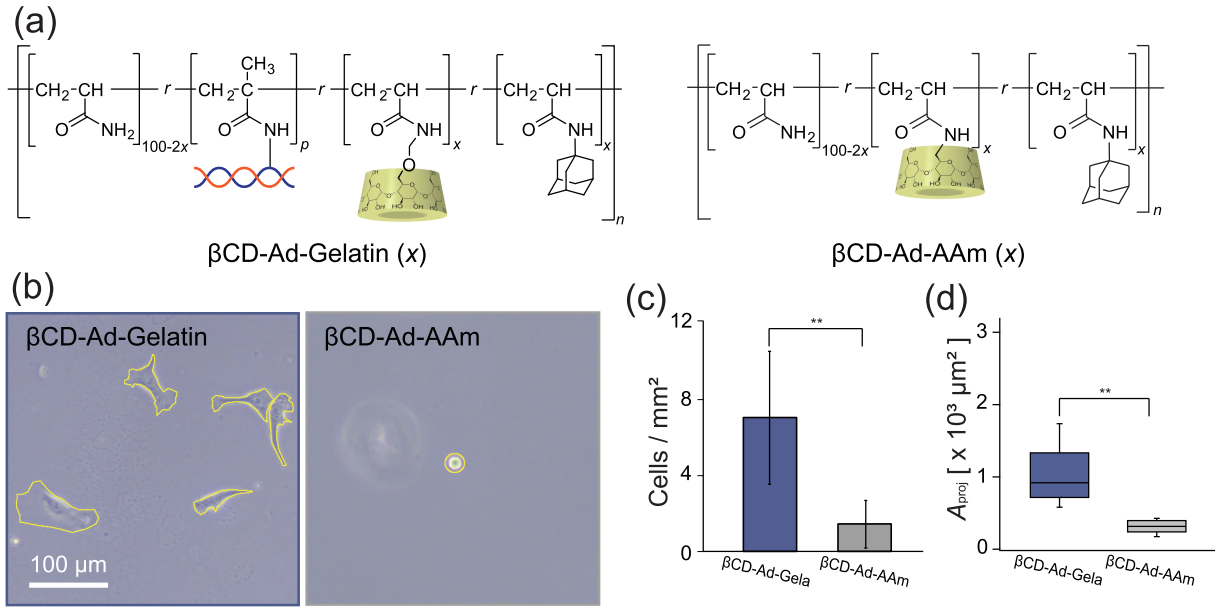

Figure 1. (a) Chemical structures of βCD-Ad-Gelatin and βCD-Ad-AAm. x is the molar fraction of host/guest monomers (x = 0−4 mol %), and p is the fraction of methacrylamide-modified gelatin (p = 0.065 mol %). (b) Phase-contrast images of C2C12 myoblasts seeded on βCD-Ad-Gelatin (left) and βCD-Ad-AAm (right) with x = 2 mol % (t = 8 h). C2C12 cells established firm adhesion on βCD-Ad-Gelatin substrates, but the adhesion on βCD-Ad-AAm was much less pronounced. The rim of the cell-substrate contact is highlighted by a yellow line. (c) Fraction of adherent cells per 1 mm^2 (N = 8 fields) and (d) projected area of a single cell A_{proj} on two substrates. N > 45 cells per condition and ** indicates p < 0.005.

$$F = 4Er^{1/2}\cdot[3(1-\nu)^2]^{-1}\cdot\delta^{3/2} \quad (1)$$

where F is the force applied to the indenter, ν = 0.5 is the Poisson's ratio assumed for hydrogels, and δ is the indentation depth.[31] The thickness of βCD-Ad-Gelatin on the glass slide was measured using a confocal laser scanning microscope (Keyence VK-X200, Osaka, Japan). Cross-sectional micrographs of the sample were obtained by confocal laser scanning at increments of 1 μm. The thickness was determined by measuring the distance between the light reflected from the top and bottom surfaces of the film. To check if swelling in the lateral direction occurred, we embedded 0.2 μm large FluoSpheres latex particles (580/605) (Thermo Fisher, Tokyo, Japan) near the surface and monitored the lateral displacement in the presence and absence of AdCOONa.[26] Unless otherwise stated, each data point is from more than three independent measurements, and the error bars in each figure correspond to the standard deviation.

2.5. Cell Culture. Mouse myoblast cells (C2C12, < 20 passages, ATCC, Manassas, Virginia) were cultured in RPMI-1640 medium supplemented with 10 wt. % of fetal bovine serum, 100 U/mL penicillin, and 100 μg/mL streptomycin. The cells were detached from the culture flasks via enzymatic digestion using trypsin−ethylenediaminetetraacetic acid (EDTA) (0.25%, Sigma) and seeded (2.7×10^3 cells/cm^2) on the substrates. The effect of free AdCOONa in the medium on the viability of C2C12 cells was evaluated using the WST assay.[21,26]

2.6. Immunohistochemistry. Prior to immunohistochemistry, the cells were pretreated with cytoskeletal buffer (CSK buffer)[32] containing 0.5% Triton X-100, 10 mM piperazine-*N*,*N*′-bis(2-ethane sulfonic acid) (PIPES, pH 6.8), 50 mM NaCl, 3 mM $MgCl_2$, and 300 mM sucrose for 1 min on ice to avoid the nonspecific signals from inactive proteins in the cytoplasm. The cells were fixed in 4% paraformaldehyde in PBS(+) buffer, requiring 15 min at room temperature. Prior to immunochemical staining, the samples were incubated with 5 wt. % bovine serum albumin (BSA, Nacalai Tesque, Kyoto, Japan) dissolved in PBS for 30 min at room temperature. For immunochemical staining, the following affinity probes and antibodies were used: mouse anti-vinculin (Sigma-Aldrich, Tokyo, Japan), goat anti-mouse IgG-Alexa Fluor 488 (Thermo Fischer, Tokyo, Japan), and phalloidin-Alexa Fluor 488 (Thermo Fisher, Tokyo, Japan). All incubations were performed in PBS containing 5 wt. % BSA for 1 h at room temperature, and rinsing was conducted with 0.01 vol % Tween 20 in PBS.

2.7. Imaging and Image Analysis. Snapshot images of the cells were taken using an inverted microscope (CKX41, Olympus, Tokyo, Japan) with a CAch 10 × PhP objective lens (Olympus). Immunofluorescence microscopy images were obtained using an inverted confocal microscope (Nikon, A1R, Tokyo, Japan) with 40 × Plan Apo (Nikon) and 60 × Plan Apo VC (Nikon) objectives. To monitor the dynamics of living cells, we took phase-contrast images every 10 min using an inverted microscope (IX71, Olympus, Tokyo, Japan) equipped with a LUCPlanFLN 20 × objective lens (Olympus) and a stage top incubator that maintains the atmosphere at 37 °C and with 5% CO_2 (Tokai Hit, Shizuoka, Japan). Morphological parameters, such as projected area A, aspect ratio AR (the ratio of major to minor axes), and circularity $C = 4\pi A/(\text{perimeter})^2$, of the adherent C2C12 cells were calculated using the ImageJ software.

2.8. Statistical Analysis. For each dataset, the normality of the distribution was tested using the Shapiro−Wilk test. When a dataset showed a non-normal distribution, the difference between different groups was assessed using the Mann−Whitney U test. Otherwise, we performed the student's t-test or Welch's t-test. Throughout this study, statistical analyses were performed using Microsoft Excel and R Open.

All data generated or analyzed during this study are included in this published article (and its Supplementary Information files).

3. RESULTS AND DISCUSSION

3.1. Gelatin Side Chains Enable Stable Cytoadhesion without Additional Surface Chemistry. Figure 1a shows the chemical structures of the gelatin-conjugated supramolecular hydrogel synthesized in this study (βCD-Ad-Gelatin) and the supramolecular hydrogel without ECM proteins used in our previous study (βCD-Ad-AAm).[26] Figure 1b shows representative phase-contrast images of C2C12 myoblast cells seeded on βCD-Ad-Gelatin and βCD-Ad-AAm. The molar fraction of host/guest monomers was set to x = 2

https://doi.org/10.1021/acsapm.1c01902
ACS Appl. Polym. Mater. 2022, 4, 2595−2603

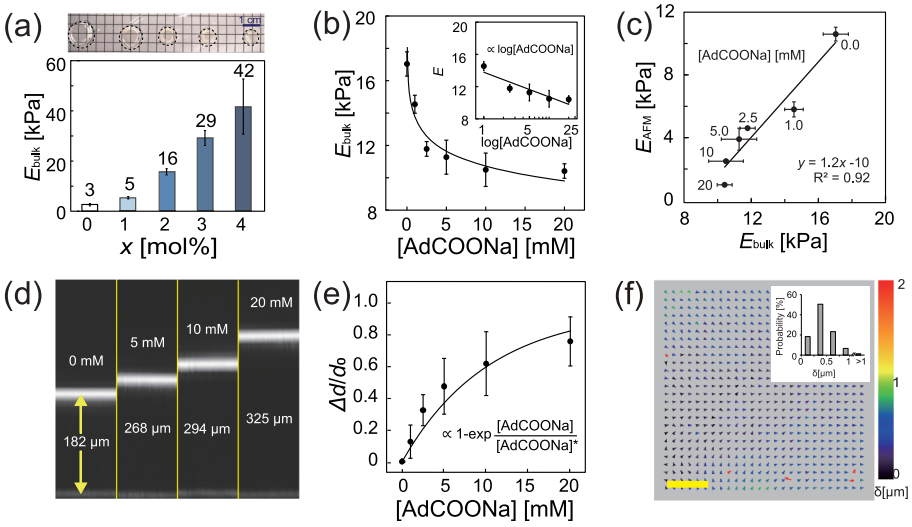

Figure 2. (a) Young's moduli of a series of βCD-Ad-Gelatin determined using a bulk creep meter E_{bulk} versus the molar fraction of host/guest monomers x. An increase in x leads to a monotonic decrease in size (upper panel) and an increase in E_{bulk} (lower panel). (b) E_{bulk} versus the concentration of free AdCOONa in solutions, [AdCOONa], and fit to $E_{bulk} \propto \log$ [AdCOONa] (solid line). (c) Young's moduli of βCD-Ad-Gelatin films determined via AFM indentation E_{AFM} show a positive correlation with E_{bulk}. (d) Cross-sections of βCD-Ad-Gelatin films at [AdCOONa] = 0−20 mM captured using a confocal microscope. (e) Swelling ratio $\Delta d/d_0$ versus [AdCOONa] and fit to an exponential function (solid line), suggesting that βCD-Ad-Gelatin films swell only in the direction perpendicular to the surface. Each dataset coincides with the mean and standard deviation from four independent experiments. (f) Lateral displacement of fluorescent beads embedded in the gel after 40 min of incubation with 5 mM AdCOONa. The histogram (inset) shows that a lateral displacement of >99% of the beads is $\delta \leq 1$ μm. Scale bar: 50 μm.

mol % for both samples to ensure that the substrate stiffness was comparable ($E_{bulk} \approx 15$ kPa).[26] C2C12 cells firmly adhered to βCD-Ad-Gelatin, exhibiting distinct spreading. On the other hand, the number of cells adherent on βCD-Ad-AAm was much less, and the cell-substrate contact remained small. Figure 1c shows the fractions of adherent cells per 1 mm^2, and Figure 1d shows the projected area of each cell A_{proj} on the two substrates. Significant differences in both the number density and the projected area indicated that the gelatin side chains of βCD-Ad-Gelatin promoted stable cell adhesion without additional surface functionalization, which validated our material design.

3.2. Fine-Adjustment of Substrate Stiffness by Supramolecular Cross-Linkers. Figure 2a shows the photographs of a series of bulk βCD-Ad-Gelatin gels and their Young's moduli E_{bulk}, wherein the molar fraction of host/guest monomers x was systematically varied. An increase in x from 0 to 4 mol % resulted in a monotonic decrease in size (upper panel) and a monotonic increase in E_{bulk} from 3 to 42 kPa (lower panel). As a previous study has shown that the formation of parallel acto-myosin bundles in differentiating myotubes was optimal at $E \sim 10$ kPa[3], we focus on gels with x = 2 mol % ($E \approx 15$ kPa) to control the adhesion and morphology of myoblasts. It should be noted that methacrylamide-modified gelatin might form chemical cross-links, but the number of cross-links remains constant. The fact that the sample containing no host-guest cross-links (x = 0) formed a stable gel with E = 3 kPa clearly indicates the presence of chemical cross-links. On the other hand, host/guest molecules in solutions competitively bind and form inclusion complexes. In the next step, we measured the bulk elastic modulus E_{bulk} of βCD-Ad-Gelatin with x = 2 mol % in the absence and presence of water-soluble AdCOONa (Figure 2b). It is notable that E sharply decreased as [AdCOONa] increased from 0 to 20 mM. As shown in the inset, the linear relationship between E_{bulk} and log[AdCOONa] suggests that the elastic modulus can be controlled by the chemical potential of free AdCOONa in solution. Because the cells were seeded on thin films (∼100 μm) for microscopy observation, we also prepared βCD-Ad-Gelatin films (see Materials and Methods) and measured Young's modulus via AFM indentation. The Young's moduli of films measured via AFM indentation E_{AFM} and bulk gels measured using a creep meter E_{bulk} measured at various [AdCOONa] are presented in Figure 2c. The positive correlation between E_{AFM} and E_{bulk} provides clear evidence that the elasticity of thin βCD-Ad-Gelatin films can also be finely adjusted by changing [AdCOONa]. As shown in Figure 2d, the thickness of the βCD-Ad-Gelatin films d monotonically increased from 182 to 325 μm as [AdCOONa] increased from 0 to 20 mM (see Supporting Information S8 for more detailed statistics from four independent measurements). Figure 2e shows the swelling ratio $\Delta d/d_0$ of βCD-Ad-Gelatin plotted as a function of [AdCOONa] in which the best fit is an exponential function (solid line), suggesting that the βCD-Ad-Gelatin films swell only in the direction perpendicular to the surface. Using particle image velocimetry, we confirmed that >99% of the fluorescently labeled latex nanoparticles embedded near the surface moved laterally with a displacement of Δx < 1 μm when [AdCOONa] was switched from 0 to 5 mM (Figure 2f). The one-dimensional swelling of films observed here is distinct from the isotropic swelling of quadratic, three-dimensional objects,[27] which can be explained by the constraint placed on the thin film, that is, the film is covalently anchored to the solid substrate.[33]

3.3. Fraction of Host/Guest Cross-Linkers Affects Adhesion of Myoblasts. In the next step, we investigated the effect of the molar fraction of host/guest monomers x on the adhesion and morphology of C2C12 myoblasts on βCD-Ad-Gelatin. Figure 3a shows representative phase-contrast microscopy images of C2C12 myoblasts after 8 h of seeding on βCD-Ad-Gelatin films. C2C12 cells seeded on the βCD-Ad-Gelatin film with x = 1 mol % have a smooth and round shape,

https://doi.org/10.1021/acsapm.1c01902
ACS Appl. Polym. Mater. 2022, 4, 2595−2603

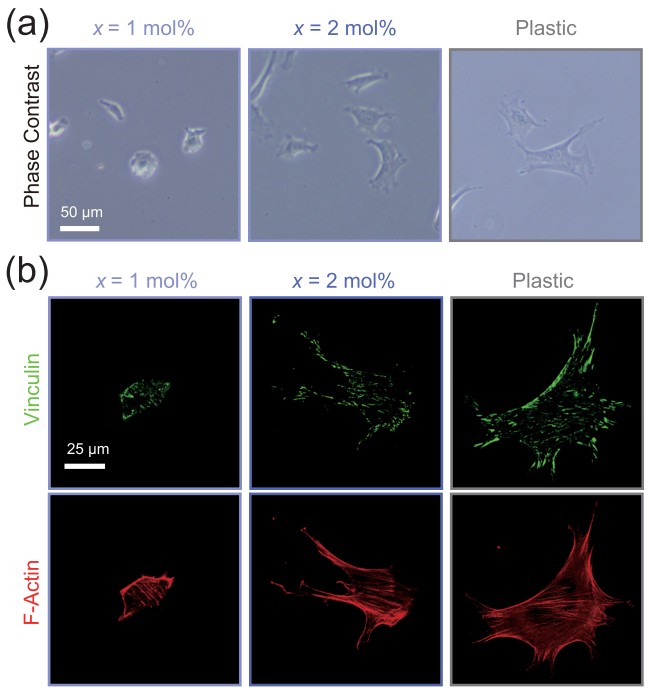

Figure 3. (a) Phase-contrast microscopy images of C2C12 myoblasts after 4 h of seeding on βCD-Ad-Gelatin with x = 1 mol % (left) and 2 mol % (middle) and on a plastic substrate (right). (b) Confocal immunofluorescence images of C2C12 with vinculin (green, upper panels) and actin (red, lower panels).

whereas C2C12 cells on the gel with x = 2 mol % exhibit pronounced spreading by contractile force generation.[34] Furthermore, to highlight the impact of substrate stiffness on cell adhesion behavior, we also collected the phase-contrast image of C2C12 cells seeded on commercially available plastic dishes that are widely used for cell culture. Compared to the βCD-Ad-Gelatin films, Young's modulus of the base material, cyclic olefin copolymer, is about five to six orders of magnitude larger ($E \sim 1$ GPa). As shown in Supporting Information S9, a statistical comparison of the projected area A_{proj} of $N > 100$ cells indicated that the median value of A_{proj} on βCD-Ad-Gelatin with x = 2 mol % ($A_{proj(x=2)} \approx 1.2 \times 10^3$ μm^2) was significantly larger than that on βCD-Ad-Gelatin with x = 1 mol % ($A_{proj(x=1)} \approx 0.5 \times 10^3$ μm^2). This finding agrees with previous studies in which an increase in the cross-linker density leads to an increase in substrate stiffness, resulting in a larger A_{proj}.[35] In fact, the corresponding values on plastic substrates ($E \sim 1$ GPa) was larger than that on hydrogels, that is, $A_{proj(plastic)} \approx 1.8 \times 10^3$ μm^2.

As the spreading of cells on substrates is driven by the polymerization of actin cytoskeletons connected to focal adhesion complexes,[36] we anticipated that the cells adapt their focal adhesions and remodel the actin cytoskeletons in response to the stiffness of contact substrates. To verify this hypothesis, we further investigated the effect of cross-linker fraction x on focal adhesions and actin cytoskeletons using confocal fluorescence microscopy. The upper panels of Figure 3b are representative confocal fluorescence images of C2C12 with anti-vinculin (green), one of the key proteins associated with focal adhesion complexes.[37] Compared with C2C12 cells on βCD-Ad-Gelatin with x = 1 mol % (left), focal adhesions on βCD-Ad-Gelatin with x = 2 mol % (middle) have a much larger size and quantity. This tendency was even more pronounced on plastic substrates (right). This agrees with previous studies, demonstrating that focal adhesions are larger and more oriented on when the substrate is stiffer.[38] The elongated, large focal adhesions near the periphery of cells recruit and activate Rho family small guanosine triphosphate-

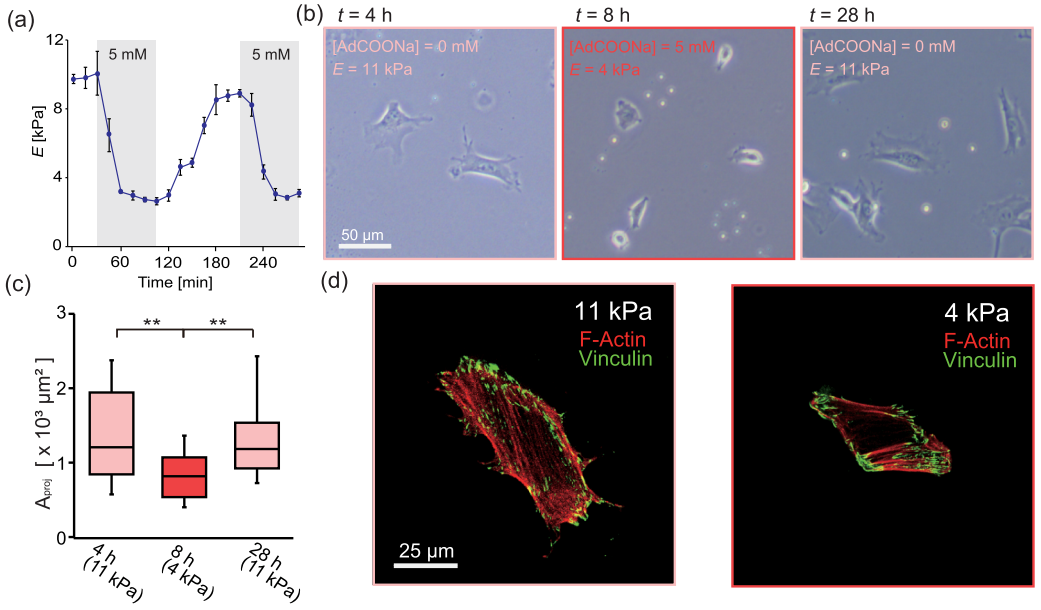

Figure 4. (a) Reversible switching of Young's modulus of βCD-Ad-Gelatin (x = 2 mol %) under the continuous exchange of the RPMI-1640 medium at 37 °C in the absence and presence of 5 mM AdCOONa monitored by in situ AFM. Flux: 0.5 mL/min. (b) Phase-contrast images of C2C12 myoblasts responding to changes in the concentration of free AdCOONa in the medium: [AdCOONa] = 0 mM (t = 4 h), 5 mM (t = 8 h), and 0 mM (t = 28 h). Medium exchange occurred at t = 4 and 8 h, shortly after image acquisition. (c) Statistical comparison of A_{proj} calculated from $N > 100$ cells out of two independent sets of experiments. ** indicates $p < 0.005$. (d) Immunofluorescence images of C2C12 cells with vinculin (green) and actin (red) in the presence and absence of AdCOONa.

https://doi.org/10.1021/acsapm.1c01902
ACS Appl. Polym. Mater. 2022, 4, 2595−2603

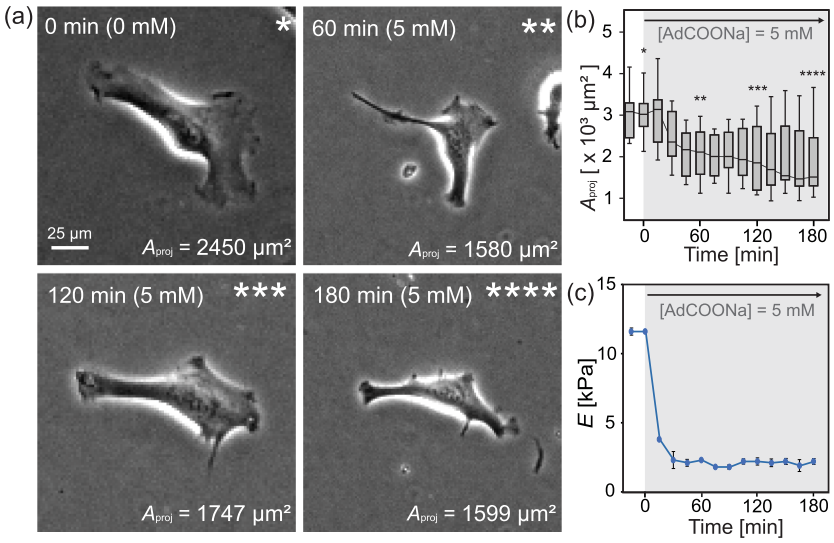

Figure 5. Dynamic adaptation of cell morphology monitored via time-lapse live cell imaging. Imaging started after 4 h of seeding when the cells reached a steady state. (a) Snapshot phase-contrast images of a representative cell taken before medium exchange (0 mM) and at 60 min (5 mM), 135 min (5 mM), and 195 min (5 mM) after medium exchange. (b) A_{proj} versus time monitored by 2 independent time-lapse experiments (N = 10 cells). (c) E_{AFM} versus t exhibit a sharp decrease upon medium exchange, reaching a steady state at t = 30 min.

binding proteins (Rho-GTPase), which act as key regulators of actin polymerization.[36]

It is also well established that focal adhesion complexes are coupled to bundles of filamentous actin, called stress fibers, and transmit information about substrate stiffness to cell nuclei via traction force.[39] Using chemically cross-linked polyacrylamide gels, Kuroda et al. reported that the differentiation of mouse mesenchymal stem cells (mMSCs) to adipocytes is regulated by actin-associated vinculin.[40] As shown in Figure 3b, immunofluorescence images of filamentous actin cytoskeletons (F-actin, red) on βCD-Ad-Gelatin with x = 2 mol % (middle) and on plastic substrates (right) follow the focal adhesion near the cell periphery, showing the "arcs" of long stress fibers. When cells are in mechanical equilibrium and do not move, the arclike stress fibers can be explained by the counterbalance between the surface tension pulling the periphery inward to reduce the adhesion area and the line tension connecting the focal adhesions by generating traction forces.[41] Conversely, such arclike features were not observed on βCD-Ad-Gelatin with x = 1 mol % (left), implying that cells do not generate contractile forces on soft hydrogel substrates.

In the following, we focus on x = 2 mol % because the elasticity in the absence of AdCOONa is close to the optimal elasticity for myotube differentiation ($E \sim 10$ kPa).[3] In fact, previous studies have shown that the further elevation of E to the noncompliant level results in the phenotype closer to those on plastic or glass ($E \sim 1$ GPa), where A_{proj} vs E can be fitted with an empirical Hill equation.[35,42]

3.4. Response of Myoblasts to Changes in Substrate Elasticity. Next, we added free AdCOONa molecules to the culture medium to characterize the response of C2C12 cells to changes in substrate elasticity, manifested in their adhesion contact and morphology. Prior to the experiments, we monitored the change in Young's modulus of βCD-Ad-Gelatin (x = 2 mol %) under the continuous exchange of RPMI-1640 medium containing [AdCOONa] = 0 and 5 mM and confirmed the reversible switching of E (Figure 4a). We also confirmed that free AdCOONa dissolved in the medium does not interfere with the viability (Supporting Information Figure S10) and adhesion (Supporting Information Figure S11) of C2C12 myoblasts. C2C12 cells were seeded on βCD-Ad-Gelatin with x = 2 mol % in AdCOONa-free medium and kept for 4 h ($E \approx 11$ kPa). After the images were taken, the medium was replaced with the medium containing [AdCOONa] = 5 mM, and the cells were incubated for another 4 h. Finally, the medium was replaced with the AdCOONa-free medium. The phase-contrast images captured at t = 4 h ([AdCOONa] = 0 mM), 8 h ([AdCOONa] = 5 mM), and 28 h ([AdCOONa] = 0 mM) are shown in Figure 4b. The shape of the C2C12 cells changed from an axially stretched shape to a smooth, roundish shape when [AdCOONa] increased from 0 to 5 mM. Notably, this morphological change was reversed when AdCOONa in the medium was depleted. Figure 4c shows the projected area of cells on "stiff" gels ([AdCOONa] = 0 mM, $E_{AFM} \approx 11$ kPa) and on soft gels $A_{proj(soft)}$ ([AdCOONa] = 5 mM, $E_{AFM} \approx 4$ kPa), indicating that this parameter is reversibly switchable. The other morphometric parameters are summarized in Supporting Information Figure S12. Immunohistochemical staining of focal adhesions (vinculin, green) and actin cytoskeletons (red) of fixed cells further confirmed the remodeling of focal adhesion complexes in response to changes in substrate elasticity (Figure 4d). To verify if ECM synthesized by cells affect cell adhesion, we compared A_{proj} of cells kept in [AdCOONa] = 0 mM with the cells experiencing the medium exchange at t = 28 h and found no significant difference (Supporting Information S13).

It is notable that the change in E, caused by a change in the density of cross-links either due to a lower x or due to the presence or absence of free AdCOONa molecules in the medium, could lead to a change in the number of density of gelatin moieties binding to integrin receptors, although we kept the amount of methacyrlamide-modified gelatin constant (Supporting Information S5). In our experimental system, it is plausible that the surface density of gelatin does not change by the addition of AdCOONa because the swelling of βCD-Ad-Gelatin occurs only in the direction perpendicular to the surface (Figure 2). On the other hand, previous studies have shown that the adherent cells deform polymer substrates with

https://doi.org/10.1021/acsapm.1c01902
ACS Appl. Polym. Mater. 2022, 4, 2595−2603

low Young's moduli, typically below 1 kPa, in the direction perpendicular to the surface.[42,43] In this case, integrin receptors might be able to bind to gelatins underneath the surface. To verify this possibility, we utilized the confocal image stacks and reconstructed the three-dimensional shape of C2C12 on the soft substrate βCD-Ad-Gelatin (x = 2 mol %) at [AdCOONa] = 5 mM ($E \approx 4$ kPa).[42] As presented in Supporting Information S14, the bottom surface of the cell follows the flat hydrogel surface, showing no clear sign of vertical substrate deformation.

To determine the kinetics of the morphological switching of cells, we took time-lapse microscopic images of the cells. Similar to the previous experiments (Figure 4), C2C12 myoblasts were seeded on βCD-Ad-Gelatin in AdCOONa-free medium for 4 h. After confirming that the cells reached a steady state by taking two successive images (Δt = 15 min), the medium was replaced with a medium containing 5 mM AdCOONa. Figure 5a shows four representative snapshot images of one C2C12 cell taken before the medium exchange ([AdCOONa] = 0 mM) and at different time points after the medium exchange ([AdCOONa] = 5 mM): 60, 135, and 195 min. Another set of snapshot images are presented in Supporting Information S15. Figure 5b shows the change in A_{proj} of 10 cells continuously monitored over time, obtained by two independent time-lapse live cell imaging experiments. The data points corresponding to the images are marked with symbols. The zone shaded in gray is the time window in which the βCD-Ad-Gelatin substrate is in the medium with [AdCOONa] = 5 mM. The projected area of the cell before the medium exchange was $A_{proj} \approx 3000\ \mu m^2$. After the medium exchange such that [AdCOONa] = 5 mM, A_{proj} started decaying over time. Figure 5c shows the change in E_{AFM} monitored via AFM indentation with the same time interval (Δt = 15 min). To compare the kinetics of E_{AFM} with that of cellular response, we used the same chamber and exchanged the medium in the same manner as we did in the live cell imaging. As shown in Figure 5c, E_{AFM} rapidly decreased and reached a steady state after 30 min, indicating that the morphological transition followed the switching of substrate elasticity. A slight delay (15−30 min) before the start of area decrease can be attributed to the time required to cancel focal adhesions. After 90 min on, A_{proj} showed a larger scatter among each other, but the general tendency was found in N = 10 cells that could be captured continuously over 180 min by two independent time-lapse experiments. It should be noted that many cells migrated out of the fields of view during imaging. As shown in Figure 4, the change in adhesion contacts and morphology can be reversed by removing AdCOONa through medium exchange. Intriguingly, we found that the kinetics of spreading was more diverse compared with that of compaction, which agrees well with our previous study using βCD-Ad-AAm functionalized with fibronectin.[22,26] This can be attributed to the fact that the kinetics of compaction is governed by actin depolymerization, which immediately starts upon the cancellation of focal adhesions, whereas the spreading of cells requires actin polymerization near the spreading fronts, establishment of near focal contacts, and formation of stable lamellipodia.

4. CONCLUSIONS

In this study, we reported a one-step synthesis of supramolecular hydrogels containing gelatin side chains in addition to host (βCD) and guest (Ad) cross-linkers, denoted as βCD-Ad-Gelatin. In contrast to the polyacrylamide-based supramolecular hydrogels with βCD/Ad side chains (βCD-Ad-AAm) used in our previous study,[26] βCD-Ad-Gelatin comprising gelatin, a ligand of integrin receptors, enables the direct culturing of myoblast cells without additional surface functionalization. Therefore, "as-prepared" hydrogels, such as βCD-Ad-Gelatin, can be used as ready-to-use cell culture substrates such that tedious surface functionalization steps with the ECM using cross-linkers, such as sulfo-SANPAH, can be circumvented. By optimizing the molar fraction of the βCD/Ad monomers x, the elasticity of the hydrogel E can be tuned in the range of 3−42 kPa, which covers the elasticity range of naturally occurring muscular tissues (∼10 kPa). We demonstrated that the elasticity of substrates constructed using βCD-Ad-Gelatin can be finely adjusted under static conditions by modifying [AdCOONa] without affecting cell viability. This allows for the reversible switching of substrate elasticity at desired step and timing $\Delta E(t)$ simply by adding and removing free guest molecules in the cell culture medium. The obtained results demonstrate that the introduction of gelatin side chains to the building blocks of supramolecular hydrogels realizes the one-step synthesis of hydrogel substrates for time-dependent modulation of focal adhesions and cell morphology with no additional surface functionalization. Recently, dynamic hydrogels with E = 1−2 kPa have been designed for 3D cell cultures, indicating the critical role of stress relaxation and bond remodeling in mechanical regulation of cells.[44,45] The application of our material design in 3D culture systems will open a large potential for the fabrication of dynamically tunable biomaterials on demand.

■ ASSOCIATED CONTENT

Supporting Information

The Supporting Information is available free of charge at https://pubs.acs.org/doi/10.1021/acsapm.1c01902.

Preparation and characterization of the materials, cell morphology, and cell viability studies (PDF)

■ AUTHOR INFORMATION

Corresponding Authors

Yoshinori Takashima − *Department of Macromolecular Science, Graduate School of Science, Osaka University, Osaka 560-0043, Japan; Institute for Advanced Co-Creation Studies, Osaka University, Osaka 565-0871, Japan;* orcid.org/0000-0002-2620-3266; Email: takasima@chem.sci.osaka-u.ac.jp

Motomu Tanaka − *Center for Integrative Medicine and Physics, Institute for Advanced Study, Kyoto University, Kyoto 606-8501, Japan; Physical Chemistry of Biosystems, Institute of Physical Chemistry, Heidelberg University, Heidelberg 69120, Germany;* orcid.org/0000-0003-3663-9554; Email: tanaka@uni-heidelberg.de

Authors

Kentaro Hayashi − *Center for Integrative Medicine and Physics, Institute for Advanced Study, Kyoto University, Kyoto 606-8501, Japan*

Mami Matsuda − *Department of Macromolecular Science, Graduate School of Science, Osaka University, Osaka 560-0043, Japan*

Nodoka Mitake − *Department of Macromolecular Science, Graduate School of Science, Osaka University, Osaka 560-0043, Japan*

Masaki Nakahata − *Department of Macromolecular Science, Graduate School of Science, Osaka University, Osaka 560-0043, Japan; Department of Materials Engineering Science, Graduate School of Engineering Science, Osaka University, Osaka 560-8531, Japan;* orcid.org/0000-0003-0397-5922

Natalie Munding − *Physical Chemistry of Biosystems, Institute of Physical Chemistry, Heidelberg University, Heidelberg 69120, Germany*

Akira Harada − *Department of Macromolecular Science, Graduate School of Science, Osaka University, Osaka 560-0043, Japan; Institute of Scientific and Industrial Research, Osaka University, Osaka 565-0047, Japan;* orcid.org/0000-0001-6177-1173

Stefan Kaufmann − *Physical Chemistry of Biosystems, Institute of Physical Chemistry, Heidelberg University, Heidelberg 69120, Germany*

Complete contact information is available at: https://pubs.acs.org/10.1021/acsapm.1c01902

Author Contributions

M.T. and Y.T. designed the research. K.H. and M.M. performed the experiments and contributed equally to the study. N.M. (Mitake), M.N., and A.H. supported the design and synthesis of the materials, S.K. and N.M. (Munding) supported the analysis of cell experiments. K.H., M.M., Y.T., and M.T. wrote the manuscript. All authors have given approval to the final version of the manuscript. K.H. and M.M. contributed equally.

Funding

Japan Society for the Promotion of Science; German Science Foundation; Nakatani Foundation.

Notes

The authors declare no competing financial interest.

■ ACKNOWLEDGMENTS

We thank P. Linke and M. Bastmeyer for inspiring discussions and insightful comments. M.N. thanks S. Sakai for helpful comments. M.M. and Y.T. thank N. Inazumi and K. Kawamura of the Analytical Instrumental Facility, Graduate School of Science, Osaka University, for supporting the ^{1}H FGMAS NMR and ATR-FT-IR experiments. This work was supported by JSPS KAKENHI (JP19H05719 to M.T. and M.N., JP20K15344 to M.N., and JP19H05721 to Y.T.) and the German Science Foundation (SPP2171-422801301 and Germany's Excellence Strategy−2082/1−390761711 to M.T.). M.T., Y.T., and M.N. thank the German−Japanese HeKKSaGOn Alliance, and M.T. thanks the Nakatani Foundation for support. We thank Edanz (https://jp.edanz.com/ac) for editing a draft of this manuscript.

■ REFERENCES

(1) Discher, D. E.; Janmey, P.; Wang, Y.-L. Tissue Cells Feel and Respond to the Stiffness of Their Substrate. *Science* **2005**, *310*, 1139−1143.

(2) Vogel, V.; Sheetz, M. Local force and geometry sensing regulate cell functions. *Nat. Rev. Mol. Cell Biol.* **2006**, *7*, 265−275.

(3) Engler, A. J.; Griffin, M. A.; Sen, S.; Bönnemann, C. G.; Sweeney, H. L.; Discher, D. E. Myotubes differentiate optimally on substrates with tissue-like stiffness: pathological implications for soft or stiff microenvironments. *J. Cell Biol.* **2004**, *166*, 877−887.

(4) Flanagan, L. A.; Ju, Y.-E.; Marg, B.; Osterfield, M.; Janmey, P. A. Neurite branching on deformable substrates. *Neuroreport* **2002**, *13*, 2411.

(5) Engler, A. J.; Sen, S.; Sweeney, H. L.; Discher, D. E. Matrix elasticity directs stem cell lineage specification. *Cell* **2006**, *126*, 677−689.

(6) Kanazawa, H.; Fujimoto, Y.; Teratani, T.; Iwasaki, J.; Kasahara, N.; Negishi, K.; Tsuruyama, T.; Uemoto, S.; Kobayashi, E. Bone marrow-derived mesenchymal stem cells ameliorate hepatic ischemia reperfusion injury in a rat model. *PLoS One* **2011**, *6*, No. e19195.

(7) Przybyla, L.; Lakins, J. N.; Weaver, V. M. Tissue Mechanics Orchestrate Wnt-Dependent Human Embryonic Stem Cell Differentiation. *Cell Stem Cell* **2016**, *19*, 462−475.

(8) Rosales, A. M.; Anseth, K. S. The design of reversible hydrogels to capture extracellular matrix dynamics. *Nat. Rev. Mater.* **2016**, *1*, 15012.

(9) Wen, J. H.; Vincent, L. G.; Fuhrmann, A.; Choi, Y. S.; Hribar, K. C.; Taylor-Weiner, H.; Chen, S.; Engler, A. J. Interplay of matrix stiffness and protein tethering in stem cell differentiation. *Nat. Mater.* **2014**, *13*, 979−987.

(10) Kidoaki, S.; Matsuda, T. Microelastic gradient gelatinous gels to induce cellular mechanotaxis. *J. Biotechnol.* **2008**, *133*, 225−230.

(11) Lambertenghi-Deliliers, G.; Orazi, A.; Luksch, R.; Annaloro, C.; Soligo, D. Myelodysplastic syndrome with increased marrow fibrosis: a distinct clinico-pathological entity. *Br. J. Haematol.* **1991**, *78*, 161−166.

(12) Gharib, S. A.; Manicone, A. M.; Parks, W. C. Matrix metalloproteinases in emphysema. *Matrix Biol.* **2018**, *73*, 34−51.

(13) Zucker, S.; Lysik, R. M.; Zarrabi, M. H.; Moll, U. M_r 92,000 Type IV Collagenase Is Increased in Plasma of Patients with Colon Cancer and Breast Cancer. *Cancer Res.* **1993**, *53*, 140−146.

(14) Stuart, M. A. C.; Huck, W. T. S.; Genzer, J.; Müller, M.; Ober, C.; Stamm, M.; Sukhorukov, G. B.; Szleifer, I.; Tsukruk, V. V.; Urban, M.; Winnik, F.; Zauscher, S.; Luzinov, I.; Minko, S. Emerging applications of stimuli-responsive polymer materials. *Nat. Mater.* **2010**, *9*, 101−113.

(15) Yan, X.; Wang, F.; Zheng, B.; Huang, F. Stimuli-responsive supramolecular polymeric materials. *Chem. Soc. Rev.* **2012**, *41*, 6042−6065.

(16) Alarcón, C. D. L.; Pennadam, S.; Alexander, C. Stimuli responsive polymers for biomedical applications. *Chem. Soc. Rev.* **2005**, *34*, 276−285.

(17) Brown, T. E.; Anseth, K. S. Spatiotemporal hydrogel biomaterials for regenerative medicine. *Chem. Soc. Rev.* **2017**, *46*, 6532−6552.

(18) Okano, T.; Yamada, N.; Okuhara, M.; Sakai, H.; Sakurai, Y. Mechanism of cell detachment from temperature-modulated, hydrophilic-hydrophobic polymer surfaces. *Biomaterials* **1995**, *16*, 297−303.

(19) Nishida, K.; Yamato, M.; Hayashida, Y.; Watanabe, K.; Yamamoto, K.; Adachi, E.; Nagai, S.; Kikuchi, A.; Maeda, N.; Watanabe, H.; Okano, T.; Tano, Y. Corneal Reconstruction with Tissue-Engineered Cell Sheets Composed of Autologous Oral Mucosal Epithelium. *New Eng. J. Med.* **2004**, *351*, 1187−1196.

(20) Tanaka, M.; Nakahata, M.; Linke, P.; Kaufmann, S. Stimuli-responsive hydrogels as a model of the dynamic cellular microenvironment. *Polym. J.* **2020**, *52*, 861−870.

(21) Yoshikawa, H. Y.; Rossetti, F. F.; Kaufmann, S.; Kaindl, T.; Madsen, J.; Engel, U.; Lewis, A. L.; Armes, S. P.; Tanaka, M. Quantitative Evaluation of Mechanosensing of Cells on Dynamically Tunable Hydrogels. *J. Am. Chem. Soc.* **2011**, *133*, 1367−1374.

(22) Inoue, S.; Frank, V.; Hörning, M.; Kaufmann, S.; Yoshikawa, H. Y.; Madsen, J. P.; Lewis, A. L.; Armes, S. P.; Tanaka, M. Live cell tracking of symmetry break in actin cytoskeleton triggered by abrupt changes in micromechanical environments. *Biomater. Sci.* **2015**, *3*, 1539−1544.

(23) Frank, V.; Kaufmann, S.; Wright, R.; Horn, P.; Yoshikawa, H. Y.; Wuchter, P.; Madsen, J.; Lewis, A. L.; Armes, S. P.; Ho, A. D.; Tanaka, M. Frequent mechanical stress suppresses proliferation of

mesenchymal stem cells from human bone marrow without loss of multipotency. *Sci. Rep.* **2016**, *6*, 24264.
(24) Kakuta, T.; Takashima, Y.; Nakahata, M.; Otsubo, M.; Yamaguchi, H.; Harada, A. Preorganized Hydrogel: Self-Healing Properties of Supramolecular Hydrogels Formed by Polymerization of Host−Guest-Monomers that Contain Cyclodextrins and Hydrophobic Guest Groups. *Adv. Mater.* **2013**, *25*, 2849−2853.
(25) Nakahata, M.; Takashima, Y.; Harada, A. Highly Flexible, Tough, and Self-Healing Supramolecular Polymeric Materials Using Host−Guest Interaction. *Macromol. Rapid Commun.* **2016**, *37*, 86−92.
(26) Hörning, M.; Nakahata, M.; Linke, P.; Yamamoto, A.; Veschgini, M.; Kaufmann, S.; Takashima, Y.; Harada, A.; Tanaka, M. Dynamic Mechano-Regulation of Myoblast Cells on Supramolecular Hydrogels Cross-Linked by Reversible Host-Guest Interactions. *Sci. Rep.* **2017**, *7*, 7660.
(27) Hippler, M.; Weißenbruch, K.; Richler, K.; Lemma, E. D.; Nakahata, M.; Richter, B.; Barner-Kowollik, C.; Takashima, Y.; Harada, A.; Blasco, E.; Wegener, M.; Tanaka, M.; Bastmeyer, M. Mechanical stimulation of single cells by reversible host-guest interactions in 3D microscaffolds. *Sci. Adv.* **2020**, *6*, No. eabc2648.
(28) Nichol, J. W.; Koshy, S. T.; Bae, H.; Hwang, C. M.; Yamanlar, S.; Khademhosseini, A. Cell-laden microengineered gelatin methacrylate hydrogels. *Biomaterials* **2010**, *31*, 5536−5544.
(29) Domke, J.; Radmacher, M. Measuring the Elastic Properties of Thin Polymer Films with the Atomic Force Microscope. *Langmuir* **1998**, *14*, 3320−3325.
(30) Rotsch, C.; Jacobson, K.; Radmacher, M. Dimensional and mechanical dynamics of active and stable edges in motile fibroblasts investigated by using atomic force microscopy. *Proc. Natl. Acad. Sci. U. S. A.* **1999**, *96*, 921−926.
(31) Lin, D. C.; Dimitriadis, E. K.; Horkay, F. Robust Strategies for Automated AFM Force Curve Analysis—I. Non-adhesive Indentation of Soft, Inhomogeneous Materials. *J. Biomech. Eng.* **2007**, *129*, 430−440.
(32) Cytoskeletal (CSK) Buffer. *Cold Spring Harb. Protoc.* **2016**, *1*, pdb.rec084301, DOI: 10.1101/pdb.rec084301.
(33) Suzuki, A.; Hara, T. Kinetics of one-dimensional swelling and shrinking of polymer gels under mechanical constraint. *J. Chem. Phys.* **2001**, *114*, 5012−5015.
(34) Murrell, M.; Oakes, P. W.; Lenz, M.; Gardel, M. L. Forcing cells into shape: the mechanics of actomyosin contractility. *Nat. Rev. Mol. Cell Biol.* **2015**, *16*, 486−498.
(35) Engler, A.; Bacakova, L.; Newman, C.; Hategan, A.; Griffin, M.; Discher, D. Substrate Compliance versus Ligand Density in Cell on Gel Responses. *Biophys. J.* **2004**, *86*, 617−628.
(36) Sackmann, E.; Tanaka, M. Critical role of lipid membranes in polarization and migration of cells: a biophysical view. *Biophys. Rev.* **2021**, *13*, 123−138.
(37) Atherton, P.; Stutchbury, B.; Jethwa, D.; Ballestrem, C. Mechanosensitive components of integrin adhesions: Role of vinculin. *Exp. Cell Res.* **2016**, *343*, 21−27.
(38) Prager-Khoutorsky, M.; Lichtenstein, A.; Krishnan, R.; Rajendran, K.; Mayo, A.; Kam, Z.; Geiger, B.; Bershadsky, A. D. Fibroblast polarization is a matrix-rigidity-dependent process controlled by focal adhesion mechanosensing. *Nat. Cell Biol.* **2011**, *13*, 1457−1465.
(39) Totaro, A.; Panciera, T.; Piccolo, S. YAP/TAZ upstream signals and downstream responses. *Nat. Cell Biol.* **2018**, *20*, 888−899.
(40) Kuroda, M.; Wada, H.; Kimura, Y.; Ueda, K.; Kioka, N. Vinculin promotes nuclear localization of TAZ to inhibit ECM stiffness-dependent differentiation into adipocytes. *J. Cell Sci.* **2017**, *130*, 989−1002.
(41) Bischofs, I. B.; Schmidt, S. S.; Schwarz, U. S. Effect of Adhesion Geometry and Rigidity on Cellular Force Distributions. *Phys. Rev. Lett.* **2009**, *103*, No. 048101.
(42) Yoshikawa, H. Y.; Kawano, T.; Matsuda, T.; Kidoaki, S.; Tanaka, M. Morphology and Adhesion Strength of Myoblast Cells on Photocurable Gelatin under Native and Non-native Micromechanical Environments. *J. Phys. Chem. B* **2013**, *117*, 4081−4088.
(43) Delanoë-Ayari, H.; Rieu, J. P.; Sano, M. 4D Traction Force Microscopy Reveals Asymmetric Cortical Forces in Migrating Dictyostelium Cells. *Phys. Rev. Lett.* **2010**, *105*, No. 248103.
(44) Chaudhuri, O.; Gu, L.; Klumpers, D.; Darnell, M.; Bencherif, S. A.; Weaver, J. C.; Huebsch, N.; Lee, H.-P.; Lippens, E.; Duda, G. N.; Mooney, D. J. Hydrogels with tunable stress relaxation regulate stem cell fate and activity. *Nat. Mater.* **2016**, *15*, 326−334.
(45) Yang, B.; Wei, K.; Loebel, C.; Zhang, K.; Feng, Q.; Li, R.; Wong, S. H. D.; Xu, X.; Lau, C.; Chen, X.; Zhao, P.; Yin, C.; Burdick, J. A.; Wang, Y.; Bian, L. Enhanced mechanosensing of cells in synthetic 3D matrix with controlled biophysical dynamics. *Nat. Commun.* **2021**, *12*, 3514.